

EIF4A3 stabilizes the expression of lncRNA AGAP2-AS1 to activate cancer-associated fibroblasts via MyD88/NF- κ B signaling

Qingqing Xu^{1,2} | Tingting Zhao² | Honghao Han³ | Jiahao Fan³ | Weiping Xie³ 

¹The First School of Clinical Medicine, Nanjing Medical University, Nanjing, People's Republic of China

²Department of Respiratory and Critical Care Medicine, Nanjing Drum Tower Hospital, Nanjing, People's Republic of China

³Department of Respiratory and Critical Care Medicine, The First Affiliated Hospital of Nanjing Medical University, Nanjing, People's Republic of China

Correspondence

Weiping Xie, Department of Respiratory and Critical Care Medicine, The First Affiliated Hospital of Nanjing Medical University, Nanjing, Jiangsu, 210029, People's Republic of China.
Email: wpxie@njmu.edu.cn

Abstract

Background: Lung cancer (LC) is a fatal malignancy and often accompanied with converting normal fibroblasts to cancer-associated fibroblasts (CAFs). Exosomal lncRNA AGAP2-AS1 has been elucidated to be a potent prognostic factor for LC, while its role in activating CAFs is largely unknown.

Methods: We first extracted exosomes from LC patients and co-cultured them with MRC5 cells to observe the state of MRC5 cells, detect AGAP2-AS1 using real-time quantitative polymerase chain reaction, and then analyze the interaction between EIF4A3 and AGAP2-AS1 using RNA pull down experiments. CCK-8 assay was used to detect cell proliferation. Transwell experiments demonstrated the regulation of MRC5 cells and, finally, the role of MyD88/NF- κ B in the downstream mechanism of EIF4A3/AGAP2-AS1 was explored by RNA interference technology and pyrrolidine-dithiocarbamic acid inhibition.

Results: We demonstrated that exosomes from the LC patients (cancer-exo) notably increased the metastatic ability of MRC-5 cells, promoting the expressions of the CAF biomarkers and lncRNA AGAP2-AS1. Overexpression of lncRNA AGAP2-AS1 prominently activated MRC-5 cells. Moreover, EIF4A3 was upregulated in the cancer-exo-treated MRC-5 cells, and EIF4A3 was verified to bind with lncRNA AGAP2-AS1 to improve its stability. The MyD88/NF- κ B signaling pathway was subsequently proved to be positively regulated by lncRNA AGAP2-AS1, and the promotive role of lncRNA AGAP2-AS1 in LC and activating CAFs was confirmed in vivo.

Conclusions: The positive feedback of EIF4A3/AGAP2-AS1/MyD88/NF- κ B signaling pathway contributed to the activation of CAFs and exacerbated LC in turn, revealing a novel regulatory axis underlying LC.

KEYWORDS

cancer-associated fibroblast, EIF4A3, lncRNA AGAP2-AS1, lung cancer, MyD88

INTRODUCTION

According to the latest data from the China Cancer Registry in 2015, the incidence and mortality of lung cancer (LC) still rank first in China among malignancies, and the incidence shows a continuous upward trend.¹ Although surgery is the optimal treatment for improving the prognosis of the patients with early LC, many patients are diagnosed in the advanced stage.² Studies in recent decades have shown that tumor progression is not only caused by the dysregulation of oncogenes or tumor

suppressor genes, but that the tumor microenvironment also exhibits great importance.³ Cancer-associated fibroblasts (CAFs) are the most vital stromal cells in the tumor microenvironment and are activated by fibroblasts in the tumor extracellular matrix.⁴ CAFs can directly contact tumor cells or secrete a variety of cytokines and metabolites in a paracrine manner to exacerbate tumors via promoting tumor growth, metastasis, and drug resistance, and the proliferation and migration ability of CAFs is stronger than that of resting fibroblasts.⁵ The activation biomarkers of CAFs are significantly increased fibroblast

activation protein (FAP) and α -smooth muscle actin (α -SMA).⁶ CAFs can also produce a variety of growth factors and pro-inflammatory cytokines, especially transforming growth factor β (TGF- β), interleukin 6 (IL-6), IL-18, collagens, and CXC chemokine ligand 12 (CXCL12) to promote tumor angiogenesis, recruiting immunosuppressive cells into the tumor microenvironment to induce tumor immune evasion.^{7,8}

Exosomes are cellular microvesicles with a diameter of 30–150 nm formed by lipid bilayer endosomal membranes.⁹ They are widely presented in body fluids, transferring proteins, nucleic acids, lipids, and their derivatives.¹⁰ The exosomal surface proteins include intraluminal proteins and transmembrane proteins such as heat shock proteins and tetraspanins. Among them, cluster of differentiation 63 (CD63) and heat shock protein 70 (HSP70) are common specific markers for exosomes.¹⁰ The ribonucleic acids contained in exosomes include messenger RNA (mRNA), microRNA (miRNA), and long non-coding RNA (lncRNA).¹¹ Exosomes fuse with the plasma membrane to transfer active biological components into target cells and regulate gene transcription and translation, thereby changing the phenotype of recipient cells.¹² Moreover, studies have found that exosomes are closely related to the progression of LC and CAFs.¹³

lncRNAs are a class of noncoding RNA transcripts consist of more than 200 nucleotides that participate in various biological processes.¹⁴ According to the positional relationship between lncRNA and protein-coding genes, lncRNAs can be divided into antisense lncRNA, intronic lncRNA, divergent lncRNA, intergenic lncRNA and enhancer lncRNA; according to the function of lncRNAs, they can be divided into signal, decoy, guide, and scaffold molecules.¹⁵ Recent studies on lncRNAs at the molecular level elucidate that the transcription of lncRNAs is time-specific and tissue-specific, and the transcripts act as signal molecules to further regulate the expression of other genes. lncRNAs can interact with DNA, RNA or proteins to epigenetically affect gene expression and serve as cellular regulators.¹⁶ lncRNAs located in the nucleus commonly exert their functions at the transcriptional level by recruiting RNA binding proteins.¹⁷ Numerous lncRNAs have been identified as carcinogenic factors in LC. For example, exosomal lncRNA AGAP2-AS1 exhibited higher levels in non-small-cell lung cancer (NSCLC) patients than in healthy people, and the expression levels of lncRNA AGAP2-AS1 were positively correlated with tumor size, lymph node metastasis, and TNM stage.¹⁸ In the present study, we hypothesized that the exosomal lncRNA AGAP2-AS1 extracted from serum of the LC patients might activate CAFs to deteriorate tumor progression, and the specific regulatory mechanism was researched.

MATERIALS AND METHODS

Isolation of exosomes

The serum samples of LC patients and healthy people were prepared to obtain the exosomes using the Exosome Isolation Kit

(UR52136; Umibio Science and Technology Group) according to the manual. Briefly, 1 ml of the serum was centrifuged for 10 min at 3000g to remove the cell debris. Then, 3 ml of PBS was used to dilute the serum and 5 ml of the Blood PureExo Solution was added to the serum and incubated for 2 h at 4°C. After that, the mixture was centrifuged at 10 000g for 60 min, and the precipitate was resuspended in 0.5 ml of PBS. The resuspended suspension was centrifuged at 12 000g for 2 min to obtain the exosome-rich supernatant. Finally, the supernatant was loaded into the upper chamber of the Exosomes Purification Filter and centrifuged to obtain the purified exosomes.

Cell culture and treatments

Human embryonic lung fibroblasts (MRC-5; CL1359-1) and A549 cell line (CL1354) were purchased from Newgain Biotech Co., Ltd. After the cells were thawed, they were respectively cultured in standard DMEM (319-005-CL) containing 10% FBS and 100 U/ml penicillin–streptomycin (all obtained from Wisent Biotech Co., Ltd.) at 37°C with 5% CO₂.

After cell confluence reached 70%–80%, MRC-5 cells were incubated with exosomes for 48 h or transfected with pcDNA3.1/lncAGAP2-AS1, pcDNA3.1/EIF4A3, sh-EIF4A3, sh-MyD88, or their negative controls (designed and synthesized by Beijing Rui Biotech Ltd.) for 48 h. Pyrrolidinedithiocarbamic acid (PDT; S1809; Beyotime Biotech) was used to inhibit the NF- κ B signaling pathway. A549 cells were transfected with pcDNA3.1/lncAGAP2-AS1 or control for 48 h before injected into the mice to induce xenografts. Transfections were carried out using Lipofectamine 2000 reagent (Invitrogen).

RNA degradation assay

MRC-5 cells in the logarithmic phase were collected and incubated with 0.5 μ M actinomycin D (Act D) for 0, 2, 4, 6, and 8 h. After incubation, the cells were collected and lysed to measure the RNA expression levels of lncRNA AGAP2-AS1 by real-time quantitative polymerase chain reaction (RT-qPCR).

Transmission electron microscopy assay

First, 10 μ l of the exosomal suspension was dropped onto a formvar-copper mesh and dried at room temperature. Next, 2% uranyl acetate was added onto the mesh and the morphology of exosomes was observed using a Cressington 108 transmission electron microscope at 80 kV after drying.

PKH67 staining assay

The exosome intake assay was conducted using a PKH67 Green Fluorescent Cell Linker Kit (PKH67GL-1KT; Sigma

Aldrich). Briefly, exosomes were stained by PKH67 solution for 10 min at 4°C. Then, the PKH67-labeled exosomes were incubated with MRC-5 cells. A fluorescence microscope (SZX7; Olympus) was used to observe the exosomes contained in MRC-5 cells after incubation for 24 h.

CCK-8 assay

MRC-5 cells were plated in 96-well plates for 24, 48, 72, and 96 h. Then, MRC-5 cells were incubated with 10 µl CCK-8 solution (Beyotime) for 2 h. The optical density was determined at 490 nm using a microplate reader (Bio-Rad).

Transwell assays

MRC-5 cells in the logarithmic growth phase were collected and starved in serum-free DMEM for 24 h. For the migration assay, transwell chambers (3422; Corning) were previously inserted into a 24-well plate. The cells were trypsinized in the serum-free DMEM and 200 µl of the cell suspension was added to the upper chambers. The bottom chambers contained 600 µl of DMEM with 2.5% FBS. After 24 h, the cells in the upper chambers were wiped off using a wet cotton swab, while the cells on the lower surface were fixed with pre-chilled methanol and stained with 0.1% crystal violet (G1064; Solarbio Technology Co., Ltd.) for 20 min. For the invasion assay, 50 µl of the Matrigel was used to coat the transwell chambers and the concentration of FBS in the bottom chamber was changed to 20%. The stained cells were observed and counted under an Olympus BX43 light microscope at a magnification of 200. Five visual fields of each well were randomly chosen.

Wound healing assay

First, 5×10^5 MRC-5 cells were seeded into a six-well plate and cultured until cell confluence reached 90%. Then, a line was scraped in the cell monolayer using the tip of a sterile micropipette. Next, the cells were rinsed with PBS to remove the cell debris and cultured in serum-free DMEM for 24 h. Images were observed and photographed under a microscope. The gaps in the wounds were measured at three random locations.

Isolation of nuclear/cytoplasmic RNA

The nucleus and cytoplasm of MRC-5 cells were isolated using a Nuclear/Cytoplasmic Separation Kit (HR0241; Balb Biotech Co., Ltd.) according to the manufacturer's instruction. Then, 5×10^5 MRC-5 cells were rinsed with PBS twice and 200 µl of Extracting Solution A was added to the cells and incubated for 30 min. After that, the cells were centrifuged and the supernatant and precipitate were separately collected. The expression levels of lncRNA AGAP2-AS1

were measured by RT-qPCR. U6 was used as the internal reference of nuclear RNA expression and GAPDH was used for cytoplasmic RNA.

Real-time quantitative polymerase chain reaction

The total RNA from MRC-5 cells was extracted using TRIzol buffer (Invitrogen). Reverse transcription and PCR amplification were carried out using a Universal RT-PCR Kit (M-MLV) (RP1100; Solarbio) on a Bio-Rad T100 Thermal Cycler. All primers were designed and synthesized by Yilaibo Biotech Co., Ltd. and GAPDH was used as internal reference. The fold changes of the RNAs were calculated according to the $2^{-\Delta\Delta Ct}$ approaches. The sequences of the primers were as follows: IL-1β forward 5'-ATGATGGCT-TATTACAGTGGCAA-3' and reverse 5'-GTCGGAGATTCGTAGCTGGA-3'; IL-6 forward 5'-ATGAACTCCTTCTC-CACAAGCGC-3' and reverse 5'-GAAGAGCCCTCAGGCTGGACTG-3'; IL-18 forward 5'-TCTTCATTGACCAAGGA AATCGG-3' and reverse 5'-TCCGGGGTGCATTATCTC-TAC-3'; α-SMA forward 5'-GTGCTGTCCCTCTATGCC TCTGG-3' and reverse 5'-GGCACGTTGTGAGTCACAC-CATC-3'; TGF-β forward 5'-CTTTGGTATCGTGGAAG-GACTC-3' and reverse 5'-AGCTGTACCAGAAATACAGC AACA-3'; CXCL12 forward 5'-GTCAGCCTGAGCTACA-GATGC-3' and reverse 5'-CTTTAGCTTCGGGTCAATGC-3'; COL1A1 forward 5'-GAGGGCCAAGACGAAGACATC-3' and reverse 5'-CAGATCACGTCATCGCACAAC-3'; COL3A1 forward 5'-CCCCTATTATTTTGGCACAACAG-3' and reverse 5'-AACGGATCCTGAGTCACAGACA-3'; COL4A1 forward 5'-CTCCACGAGGAGCACAGC-3' and reverse 5'-CCTTTTGTCCCTTCACTCCA-3'; lncRNA AGAP2-AS1 forward 5'-TACCTTGACCTTGCTGCTCTC-3' and reverse 5'-TGTCCTTAATGACCCCATCC-3'; EIF4A3 forward 5'-CTCTCCGCGGACTCTGAAT-3' and reverse 5'-CGCTGG TCTCGAATTCCACT-3'; GAPDH forward 5'-ACCCACTC CTCCACCTTTGAC-3' and reverse 5'-TGTTGCTGTAGCC AAATTTCGTT-3'.

Western blotting assay

Total proteins were extracted from MRC-5 cells and xenografts using RIPA buffer (WB020; MultiSciences Biotech Co., Ltd.). The concentrations of the proteins were measured by a BCA Kit (70-EK1105-48; MultiSciences). In brief, the protein was loaded on 10% SDS-PAGE (S1051-500; Solarbio) and separated for 30 min. Next, the proteins were transferred onto PVDF membranes (10 600 021; Cytiva) for 90 min and blocked with 5% skim milk for 1 h. The primary antibodies were then incubated with the PVDF membranes, including anti-HSP70 (1:1000; 70R-34 918; Fitzgerald), anti-CD63 (1:1000; 70R-10 168; Fitzgerald), anti-FAP (1:1000; 20R-FR012; Fitzgerald), anti-α-SMA (1:1000; ab244177; Abcam), anti-EIF4A3 (1:500; ab32485; Abcam), anti-p-NF-κB

(1:1000; BS4737; Bioworld), anti-NF- κ B (1:1000; ab283716; Abcam), anti-GAPDH (1:1000; ab8245; Abcam), and anti- β -actin (1:1000; ab8226; Abcam). GAPDH and β -actin were used to normalize protein expression levels. After incubation with the primary antibodies, the membranes were incubated with the anti-IgG secondary antibody (1:2000; ab248512; Abcam) at room temperature for 2 h. Finally, the protein bands were developed using ECL Kit (AS16-ECL-SN; Agrisera).

RNA pull-down

RNA pull-down assay was performed by an RNA pull-down kit (KT103-01; Guangzhou Saicheng Biotech Co., Ltd.) following the manual. In brief, 4×10^7 MRC-5 cells were lysed and centrifuged to collect the supernatant. The magnetic beads (50 μ l) were conjugated with biotinylated lncRNA AGAP2-AS1 probes and incubated with the supernatant (100 μ l) at 4°C overnight. Next, the beads were eluted from the RNA-protein complex. The proteins were resolved in SDS-PAGE and detected by western blotting assay.

RNA binding protein immunoprecipitation assay

RNA Binding Protein Immunoprecipitation Assay Kit (KT102-01; Guangzhou Saicheng Biotech Co., Ltd.) was applied to carry out an RNA binding protein immunoprecipitation (RIP) assay following the instructions. Briefly, 4×10^7 MRC-5 cells were lysed and centrifuged, after which 100 μ l of supernatant was collected to incubate with the magnetic beads. The magnetic beads were previously conjugated with anti-EIF4A3 antibodies (1:1000; ab32485; Abcam) and control anti-IgG antibodies. The magnetic beads were eluted and the RNA complex was purified to obtain the RNA for RT-qPCR analysis.

Tumorigenicity assay

Fifteen BLAB/c 6-week-old male nude mice (21 ± 2 g) were obtained from Jiangsu ALF Biotechnology Co., Ltd. The mice were housed in pathogen-free conditions, with the temperature maintained at $22 \pm 2^\circ\text{C}$, 50%–60% humidity, 12 h dark/light cycle, and freely available food and water. Then, 1×10^6 recombinant A549 cells were subcutaneously injected into the flanks of the mice to induce the xenografts. The tumor volumes were measured every 3 days following the formula $V = LS^2/2$, where L is the long diameter and S is the short diameter. After 4 weeks of induction, the mice were sacrificed by 150 mg/kg pentobarbital i.v., and the xenografts were resected and weighed. All the experiments were approved by the Ethics Committee of Nanjing Medical University (approval no. IACUC-2206046).

Immunofluorescence

The tumors were embedded in paraffin and sliced. After dewaxed, rehydrated and antigen retrieval, the sections were permeated by 0.2% Triton X-100 blocked by 5% BSA for 1 h. Next, the sections were incubated with the primary anti-FAP (1:1000; 20R-FR012; Fitzgerald) and anti- α -SMA (1:1000; ab244177; Abcam) antibodies at 4°C overnight. Then, the sections were incubated with secondary goat anti-rat IgG-iFluor 488 antibodies (CM008-10A2F; Chamot Biotech Co., Ltd.) at 37°C for 1 h and counter-stained with DAPI for 15 min. A ZEISS LSM 9 laser confocal microscope was used to observe the fluorescently-labeled sections.

Statistical analysis

Every assay was repeated for three independent experiments. GraphPad Prism (v9.0.0.121; GraphPad Software, Inc.) was used to analyze the data. All data were presented as the mean \pm SD. Student t -test was used to calculate the statistical differences between the two groups. Duncan's test was used for post-hoc test. ANOVA was applied for multiple groups. The value of $p < 0.05$ was deemed statistically significant.

RESULTS

Exosomes isolated from LC patients observably activated MRC-5 cells

To explore whether exosomes isolated from the LC patients were capable of activating CAFs, we incubated the exosomes with MRC-5 cells and determined the cellular functions. As Figure 1a shows, the exosomes isolated from both LC patients (cancer-exo) and healthy participants (control-exo) exhibited round shapes under transmission electron microscopy. Furthermore, control-exo and cancer-exo were HSP70- and CD63-positive (Figure 1b), authenticating the nature of the exosomes. After 24 h of incubation, PKH67-labeled exosomes (green fluorescence) could enter MRC-5 cells (Figure 1c). CCK-8 assay showed that cancer-exo promoted MRC-5 cell proliferation (Figure 1d). In addition, compared with control-exo, cancer-exo significantly promoted the migration and invasion of MRC-5 cells (Figure 1e,f). The wound-healing rate of the cancer-exo group was consistently increased (Figure 1g,h). Moreover, the levels of CAF biomarkers IL-1 β , IL-6, IL-18, α -SMA, TGF- β , CXCL12, and collagens (COL1A1, COL3A1, COL4A1) were all notably elevated by cancer-exo (Figure 1i,j). Similarly, the protein levels of FAP and α -SMA were increased (Figure 1k). These results demonstrate that cancer-exo could activate MRC-5 cells.

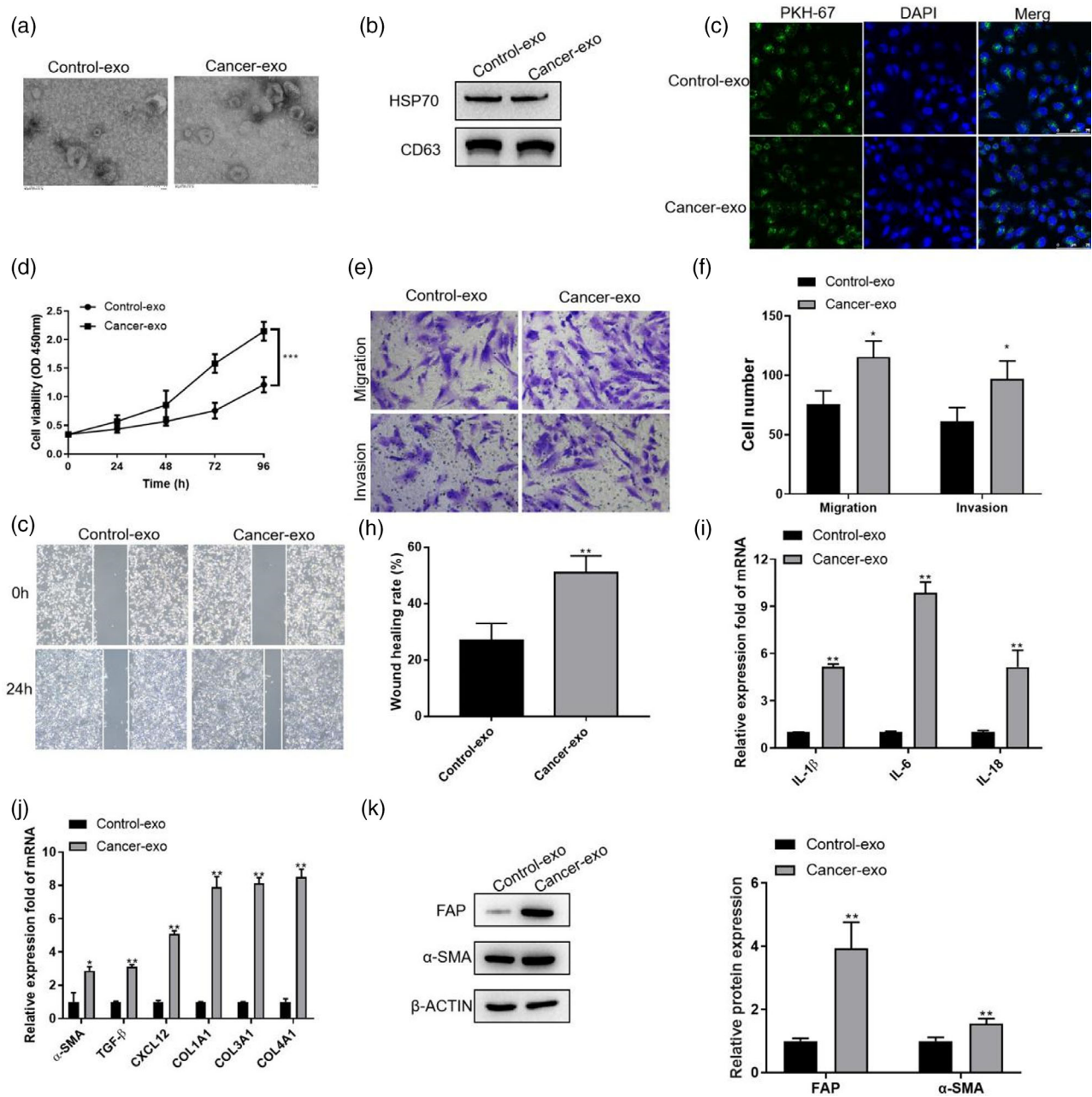


FIGURE 1 Exosomes isolated from lung cancer (LC) patients activated MRC-5 cells. (a) transmission electron microscopy images of the exosomes isolated from the serum of LC patients and healthy participants. (b) The protein bands of HSP70 and CD63 in control-exo and cancer-exo. (c) Fluorescence images of MRC-5 cells. The exosomes were labeled with PKH-67 and co-cultured with MRC-5 cells for 24 h. (d) CCK-8 assay was used to assess the viability of MRC-5 cells after co-culture with control-exo or cancer-exo. (e) and (f) After the transwell assay was performed, the migrated and invaded MRC-5 cells were captured and counted after co-culture with control-exo or cancer-exo. (g) and (h) Wound healing assay was carried out in the exosome-treated MRC-5 cells. (i) The mRNA expression levels of IL-1 β , IL-6, and IL-18 in MRC-5 cells after treatment with the exosomes. (j) The mRNA expression levels of α -smooth muscle actin (α -SMA), TGF- β , CXCL12, COL1A1, COL3A1, and COL4A1 in MRC-5 cells after treatment with the exosomes. (k) The protein levels of fibroblast activating protein and α -SMA in MRC-5 cells were determined by western blotting assay. Three independent experiments were performed for each assay. * $p < 0.05$, ** $p < 0.01$

Overexpression of AGAP2-AS1 contributed to MRC-5 activation

According to the previous finding, lncRNA AGAP2-AS1 was promising biomarkers for LC in the serual exosomes.¹⁸ RT-qPCR was used to assess lncRNA AGAP2-AS1

in control-exo and cancer-exo. The results showed that compared to the control-exo group, the level of AGAP2-AS1 was significantly increased in cancer-exo (Figure 2a). Hence, we hypothesized that lncRNA AGAP2-AS1 might play promotive roles in activating CAFs. After co-culturing the exosomes with MRC-5 cells, we

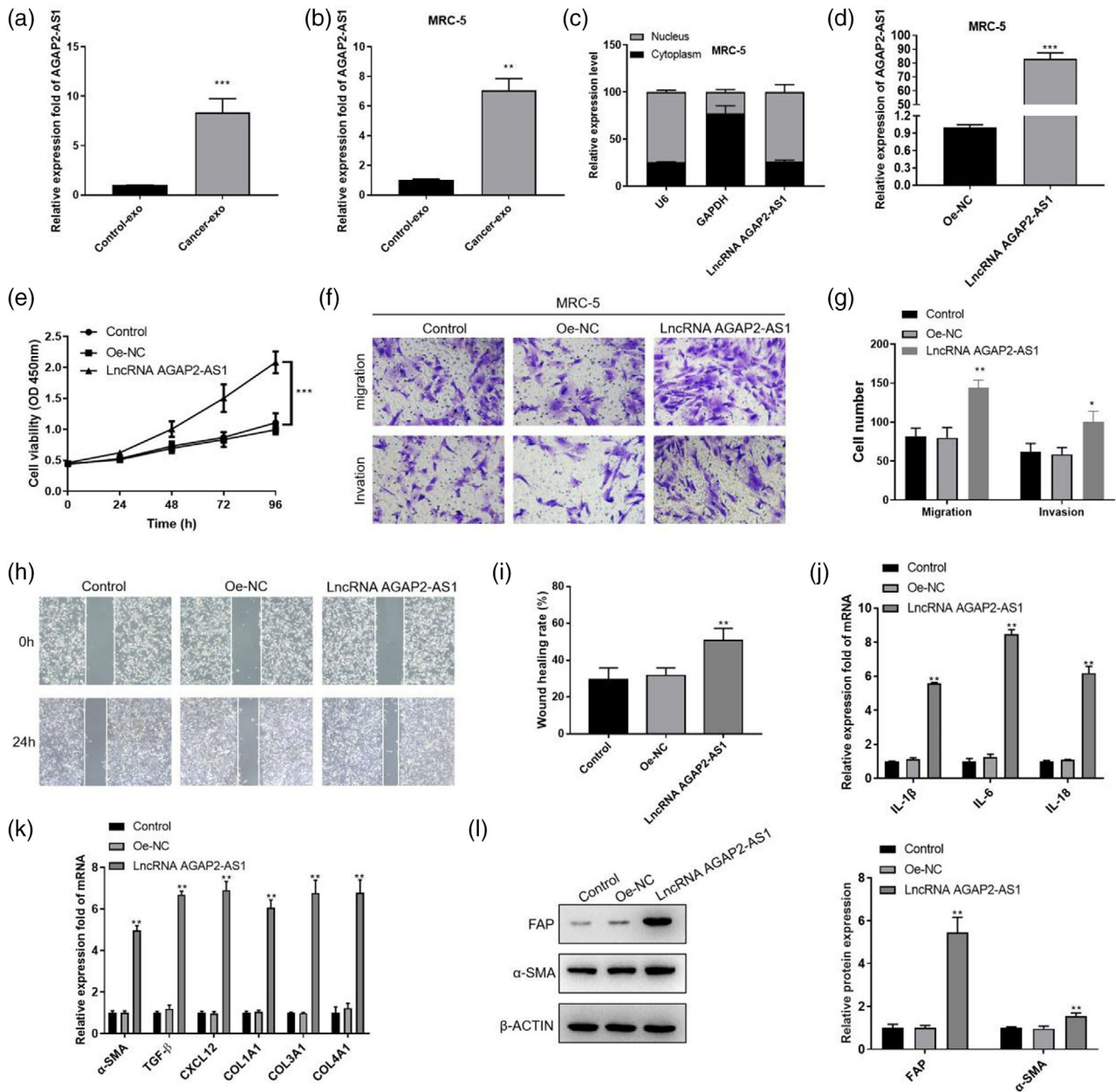


FIGURE 2 AGAP2-AS1 contributed to MRC-5 activation. (a) The expression level of AGAP2-AS1 in control-exo and cancer-exo was measured by RT-qPCR. (b) The expression level of AGAP2-AS1 in the exosome-treated MRC-5 cells was measured by RT-qPCR. (c) The proportions of nuclear and cytoplasmic AGAP2-AS1 were determined in MRC-5 cells. (d) The expression levels of AGAP2-AS1 in MRC-5 cells after transfection with AGAP2-AS1 overexpression plasmids. (e) CCK-8 assay was used to assess the viability of MRC-5 cells after transfection with AGAP2-AS1 overexpression plasmids. (f) and (g) The migrated and invaded cells were captured and counted after AGAP2-AS1 was overexpressed in MRC-5 cells. (h) and (i) Wound healing rates of MRC-5 cells were calculated after AGAP2-AS1 was overexpressed. (j) and (k) mRNA expression levels of the referred cytokines were detected in the AGAP2-AS1-overexpressed MRC-5 cells. (l) The protein levels of fibroblast activating protein and α -smooth muscle actin in the AGAP2-AS1-overexpressed MRC-5 cells. Three independent experiments were performed for each assay. * $p < 0.05$, ** $p < 0.01$, *** $p < 0.001$

observed that cancer-exo markedly enhanced the level of AGAP2-AS1 in MRC-5 cells (Figure 2b). In addition, AGAP2-AS1 was mainly located in the nucleus of MRC-5 cells (Figure 2c). Transfection of AGAP2-AS1 overexpression plasmids (AGAP2-AS1 OE) into MRC-5 cells prominently increased the expression level of AGAP2-AS1 (Figure 2d). AGAP2-AS1 OE also contributed to MRC-5 cell proliferation (Figure 2e). In addition, AGAP2-AS1 OE

notably promoted the metastatic ability of MRC-5 cells, which was proved by the increased number of migrated/invaded cells and the wound healing rate (Figure 2f-i). The mRNA expression levels of CAF biomarkers and the protein levels of FAP and α -SMA were also enhanced after AGAP2-AS1 was transfected into MRC-5 cells (Figure 2j-l). Altogether, these findings demonstrate that AGAP2-AS1 is an efficient activator of MRC-5 cells.

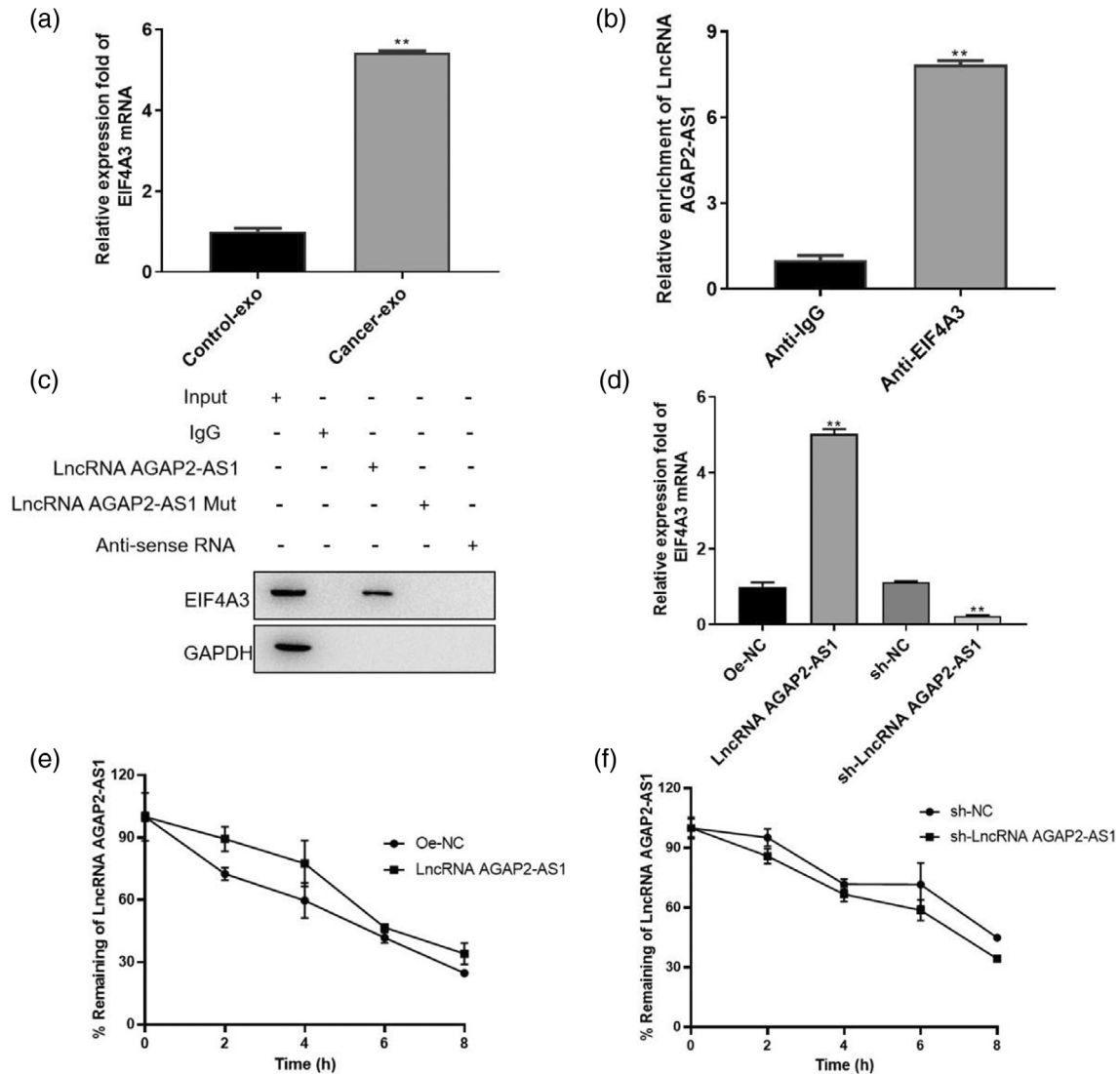


FIGURE 3 EIF4A3 was the binding protein of AGAP2-AS1. (a) The mRNA expression levels of EIF4A3 in the exosome-treated MRC-5 cells. (b) RNA binding protein immunoprecipitation and (c) RNA pull-down assays were conducted to confirm the interaction between EIF4A3 and AGAP2-AS1. (d) The mRNA expression levels of EIF4A3 in MRC-5 cells transfected with AGAP2-AS1 overexpression or sh-LncRNA AGAP2-AS1. The stability of AGAP2-AS1 in MRC-5 cells was determined after actinomycin treatment. (e) EIF4A3 overexpression or (f) sh-EIF4A3 was used to treat MRC-5 cells. Three independent experiments were performed for each assay. ** $p < 0.01$

EIF4A3 bound to AGAP2-AS1 to inhibit its degradation

To ulteriorly investigate the mechanism underlying the promotive role of AGAP2-AS1 on activating MRC-5 cells, the RNA binding proteins of AGAP2-AS1 were predicted using Starbase (<http://starbase.sysu.edu.cn/rbpClipRNA.php?source=lncRNA>), and the mRNA level of EIF4A3 was significantly increased in the cancer-exo-treated MRC-5 cells (Figure 3a). Hence, we subsequently examined the interaction between AGAP2-AS1 and EIF4A3. RIP results showed that anti-EIF4A3 antibodies enriched a prominent higher level of AGAP2-AS1 (Figure 3b) and AGAP2-AS1 notably enriched EIF4A3 proteins (Figure 3c). AGAP2-AS1 OE markedly elevated the mRNA level of EIF4A3, while

knockdown of AGAP2-AS1 showed the reverse result (Figure 3d). Furthermore, EIF4A3 enhanced the stability of AGAP2-AS1 (Figure 3e), but inhibition of EIF4A3 decreased the stability (Figure 3f). Altogether, the results indicate that AGAP2-AS1 is positively correlated with EIF4A3.

AGAP2-AS1 is functionally related to EIF4A3 in activating MRC-5 cells

The functional relationship between AGAP2-AS1 and EIF4A3 was subsequently examined. Depletion of EIF4A3 reversed the increased number of proliferative, migrated, and invaded cells induced by AGAP2-AS1; however, overexpression of EIF4A3 enhanced the promotive function of

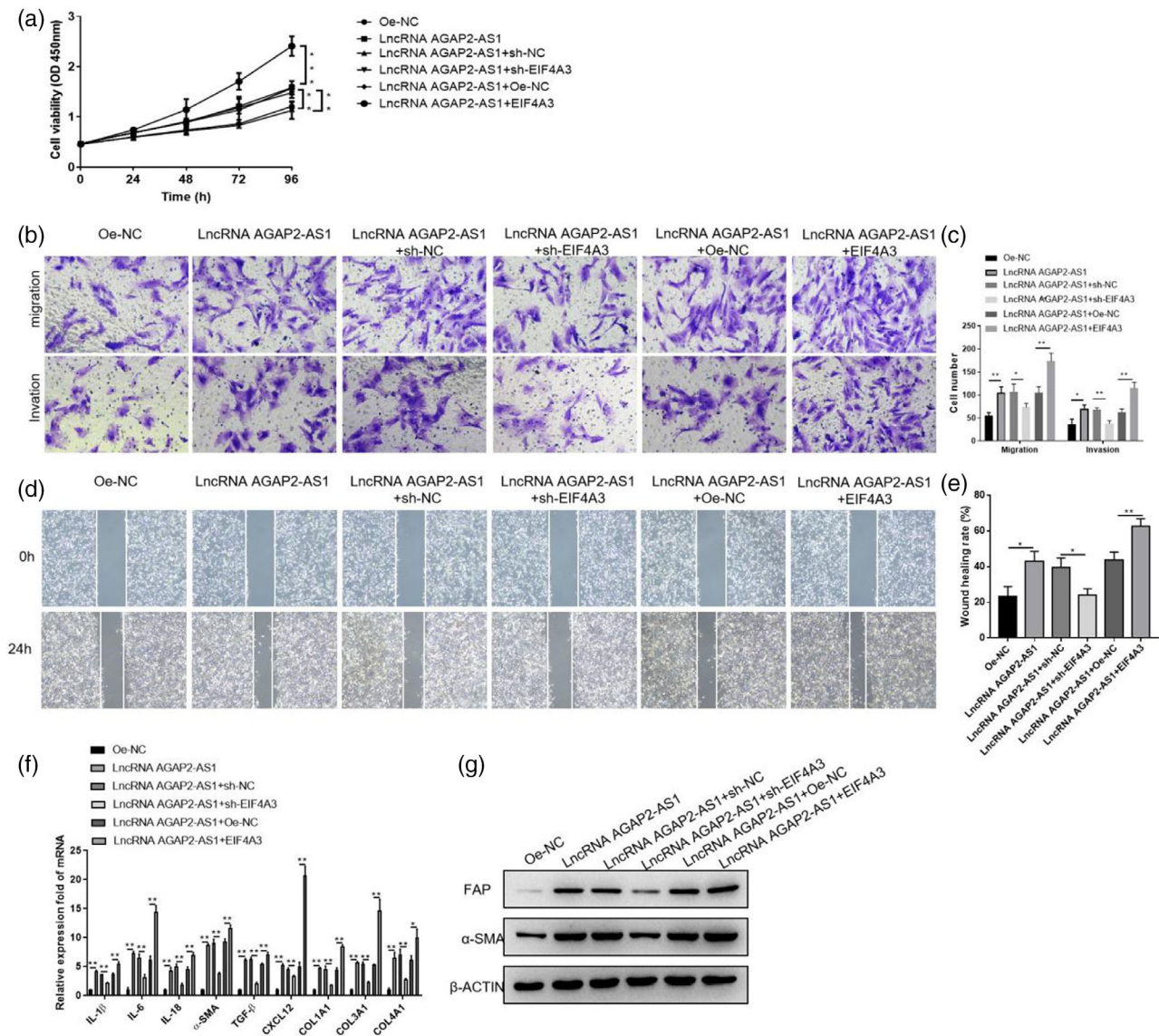


FIGURE 4 AGAP2-AS1 was functionally related to EIF4A3 in activating MRC-5 cells. (a) CCK-8 assay was used to assess the viability of MRC-5 cells. (b) and (c) Migrated and invaded MRC-5 cells analyzed by transwell assay were counted after the indicated treatments. (d) and (e) Wound healing rates were calculated after 24 h of culture. MRC-5 cells were transfected with the referred vectors. (f) mRNA expression levels of the listed cytokines in MRC-5 cells underwent the indicated transfections. (g) The protein expression levels of fibroblast activating protein and α -smooth muscle actin in MRC-5 cells transfected with the indicated vectors. Three independent experiments were performed for each assay. * $p < 0.05$, ** $p < 0.01$

AGAP2-AS1 on cell proliferation and metastasis (Figure 4a–c). The results of the wound healing assay exhibited the similar trend with the transwell assay (Figure 4d,e). Moreover, the mRNA levels of the indicated cytokines and collagens were reduced after EIF4A3 was downregulated, but increased when EIF4A3 was overexpressed (Figure 4f). Similar changes were observed in the protein levels of FAP and α -SMA (Figure 4g).

MyD88/NF- κ B is the target signaling pathway of AGAP2-AS1 in MRC-5 cells

As a previous study demonstrated, MyD88 was the downstream target of AGAP2-AS1 in breast cancer cells, and the NF- κ B signaling pathway was further activated by MyD88.¹⁹

Hence, we intended to verify the regulatory axis in MRC-5 cells. The mRNA expression of MyD88 in MRC-5 cells was prominently elevated after cancer-exo treatment (Figure 5a). Additionally, AGAP2-AS1 positively regulated the mRNA level of MyD88 (Figure 5b). The phosphorylated-NF- κ B signaling pathway was markedly enhanced by AGAP2-AS1, while knockdown of MyD88 inhibited the activation of NF- κ B and neither AGAP2-AS1 nor sh-MyD88 had a significant influence on the total NF- κ B signaling pathway (Figure 5c). Likewise, sh-MyD88 reversed the effects of AGAP2-AS1 on cell proliferation, migration, invasion, and wound healing. PDTC, an inhibitor of the NF- κ B signaling pathway, showed a similar function with sh-MyD88 (Figure 5d–h). sh-MyD88 prominently reduced the mRNA levels of the indicated cytokines that were enhanced by

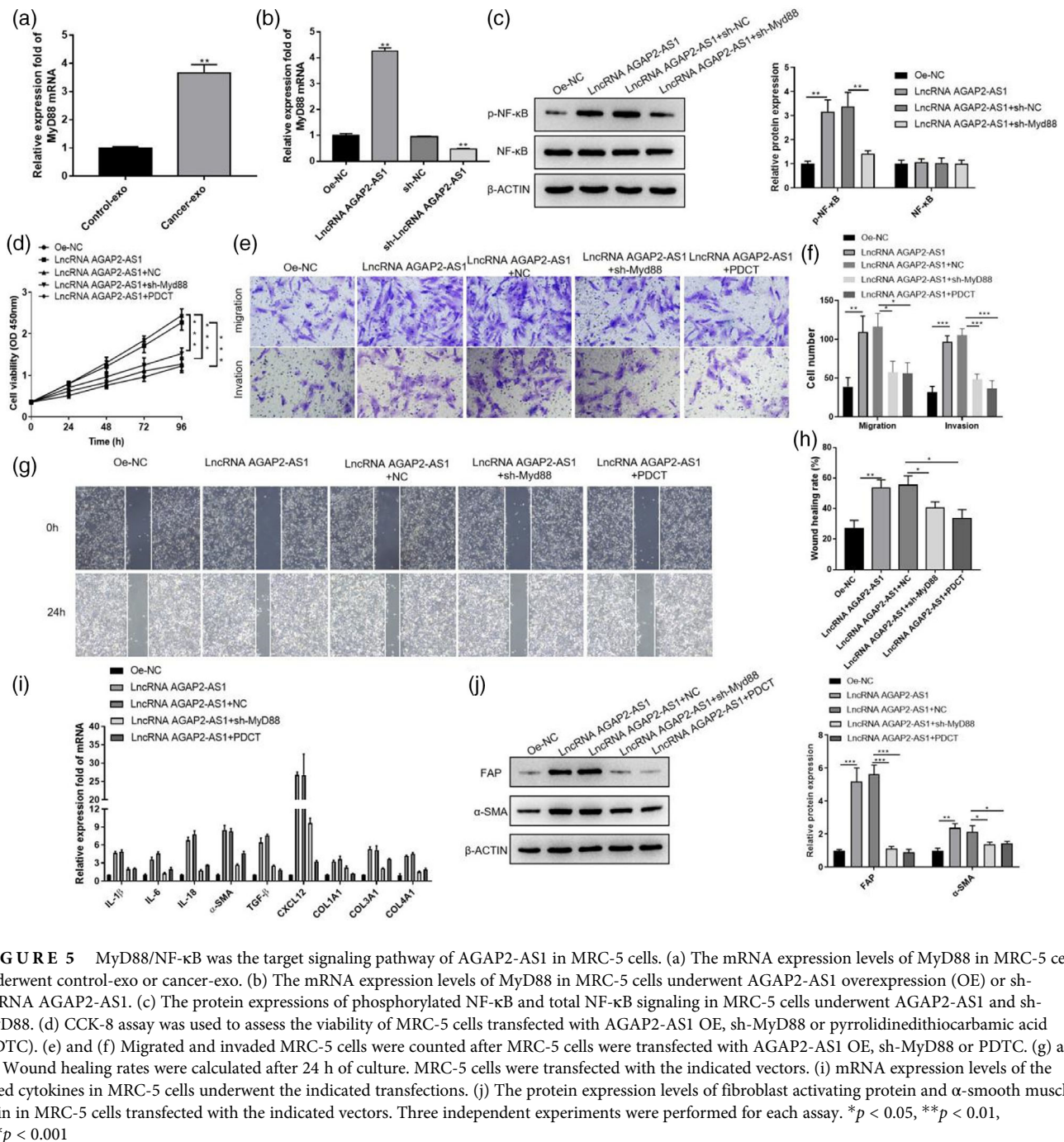


FIGURE 5 MyD88/NF- κ B was the target signaling pathway of AGAP2-AS1 in MRC-5 cells. (a) The mRNA expression levels of MyD88 in MRC-5 cells underwent control-exo or cancer-exo. (b) The mRNA expression levels of MyD88 in MRC-5 cells underwent AGAP2-AS1 overexpression (OE) or sh-lncRNA AGAP2-AS1. (c) The protein expressions of phosphorylated NF- κ B and total NF- κ B signaling in MRC-5 cells underwent AGAP2-AS1 and sh-MyD88. (d) CCK-8 assay was used to assess the viability of MRC-5 cells transfected with AGAP2-AS1 OE, sh-MyD88 or pyrrolidinedithiocarbamic acid (PDTC). (e) and (f) Migrated and invaded MRC-5 cells were counted after MRC-5 cells were transfected with AGAP2-AS1 OE, sh-MyD88 or PDTC. (g) and (h) Wound healing rates were calculated after 24 h of culture. MRC-5 cells were transfected with the indicated vectors. (i) mRNA expression levels of the listed cytokines in MRC-5 cells underwent the indicated transfections. (j) The protein expression levels of fibroblast activating protein and α -smooth muscle actin in MRC-5 cells transfected with the indicated vectors. Three independent experiments were performed for each assay. * $p < 0.05$, ** $p < 0.01$, *** $p < 0.001$

AGAP2-AS1 (Figure 5i). Similar results were observed in the protein levels of FAP and α -SMA (Figure 5j). Taken together, the results prove the AGAP2-AS1/MyD88/NF- κ B positive feedback in activating MRC-5 cells.

AGAP2-AS1 played a promotive role in LC and activating CAFs in vivo

The oncogenic role of AGAP2-AS1 was examined in nude mice (Figure 6a). Tumor growth was observably facilitated by AGAP2-AS1, as evident by the increased tumor volume

(Figure 6b) and weight (Figure 6c). The immunofluorescence images show that AGAP2-AS1 promoted the production of α -SMA (Figure 6d) and FAP (Figure 6e) in the xenografts. Consistently, the protein expression levels of α -SMA and FAP were elevated by AGAP2-AS1 (Figure 6f).

DISCUSSION

CAFs are an important part of the tumor microenvironment and play an important role in the genesis and development of tumors.⁸ Studies have shown that CAFs are mainly

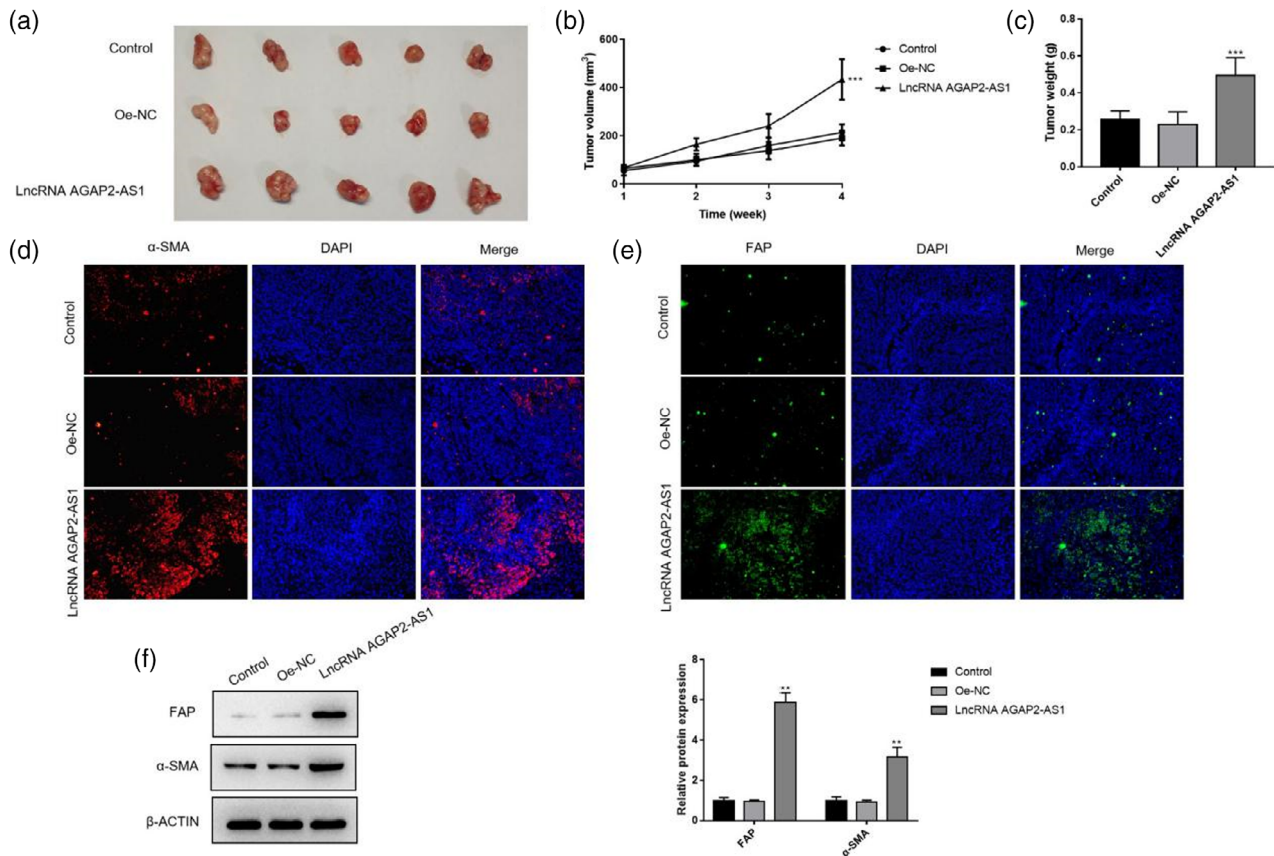


FIGURE 6 AGAP2-AS1 played a promotive role in lung cancer and activating cancer-associated fibroblasts in vivo. (a) The xenografts were resected from the mice after 4 weeks of induction. A549 cells transfected with AGAP2-AS1 overexpression (OE) or OE-control were injected into the mice to generate the xenografts. (b) Tumor volumes and (c) weights were measured in the different groups of mice. The accumulation of (d) α -smooth muscle actin (α -SMA) (red fluorescence) and (e) fibroblast activating protein (FAP) (green fluorescence) were observed via immunofluorescence assay. (f) The protein expression levels of α -SMA and FAP were determined in the xenografts. $**p < 0.01$, $***p < 0.001$

transformed from local tissue native fibroblasts.^{20,21} The transformation of CAFs is regulated by the tumor microenvironment. Exosomes play vital roles in intercellular communication through transmitting bioactive compounds.¹⁰ In recent years, the communication of exosomes between tumor cells and fibroblasts has become a focus of research. Several studies have reported that tumor-derived exosomes promote tumor growth and metastasis by inducing the formation of CAFs.²² For instance, exosomes from breast cancer cells induced the activation of CAFs through the transfer of miR-146a, thus promoting tumor invasion and metastasis.^{22,23} In the present study, we also found that exosomes from LC patients observably activated CAFs.

In LC, exosomes have been proven to exert various functions rely on the lncRNAs they carried. AGAP2-AS1 was first identified in NSCLC as an onco-lncRNA.²⁴ To date, the oncogenic role of AGAP2-AS1 has been verified in numerous malignancies. For example, AGAP2-AS1 was upregulated in hepatocellular carcinoma (HCC) tissues and cell lines, and it promoted the expression of ANXA11 through sponging miR-16-5p to exacerbate the malignant behaviors of HCC cells.²⁵ In glioma, AGAP2-AS1 targeted for miR-15a/b-5p to increase the level of HDGF, and the Wnt/ β -catenin

signaling pathway was further activated to accelerate the proliferation of glioma cells.²⁶ AGAP2-AS1 sponged for miR-497 in colorectal cancer (CRC) cells, upregulating FGFR1, and thereby promoted the progression of CRC.²⁷ Furthermore, M2 macrophage-derived exosomal AGAP2-AS1 enhances radiotherapy immunity in LC.²⁸ Exosomal lncRNA AGAP2-AS1 is one of the promising biomarkers for LC, although whether or not it possesses promotive function on activating CAFs is not clearly defined. Hence, we investigated the impact of exosomal AGAP2-AS1 on MRC-5 cells and uncovered the regulatory mechanism of AGAP2-AS1. Our original data demonstrated that AGAP2-AS1 was upregulated in MRC-5 cells after co-culture with exosomes isolated from LC patients.

As well as serving as a ceRNA for miRNAs, AGAP2-AS1 could also bind to RNA binding proteins (RBPs) to regulate gene expression at the transcriptional level. For instance, overexpression of AGAP2-AS1 promoted cell growth and invasion of gastric cancer cells. This carcinogenic function was achieved by binding to LSD1 and EZH2, the complex suppressed CDKN1A and E-cadherin transcription.²⁹ AGAP2-AS1 bound to CREB-binding protein and the complex enriched H3K27ac at the promoter region of MyD88,

thus increasing the production of MyD88; increased MyD88 further activated NF- κ B signaling and aggravated breast cancer.¹⁹ Moreover, AGAP2-AS1 suppressed the transcription of ANKRD1 and ANGPTL4 through recruiting EZH2, thereby deteriorating pancreatic cancer,³⁰ whereas AGAP2-AS1 was poorly discussed in activating CAFs. In the current study, we found that exosomes from LC patients could activate MRC-5 cells and significantly upregulate AGAP2-AS1 in MRC-5 cells. Our data first demonstrated the activating function of AGAP2-AS1 on LC-derived CAFs and the underlying mechanism, supplementing the biological role of this oncogenic lncRNA.

EIF4A3 protein belongs to the DEAD box protein family and is a nuclear matrix protein.³¹ Commonly, EIF4A3 is researched as a RBP for lncRNA in oncology. On one hand, EIF4A3 binds to lncRNA to further stabilize the mRNA of the downstream target gene. Song et al.³² elucidated that lncRNA CASC11 recruited EIF4A3 to stabilize the mRNA of E2F1, and the increased level of E2F1 further activated the NF- κ B signaling and PI3K/AKT/mTOR pathway to aggravate hepatocellular carcinoma. In addition, LINC01232 was found to recruit EIF4A3 to increase the mRNA stability of TM9SF2, and this LINC01232/EIF4A3/TM9SF2 axis promoted pancreatic adenocarcinoma.³³ Furthermore, LINC00667 was revealed to be a tumor promoter through recruiting EIF4A3 to stabilize VEGFA mRNA.³⁴ On the other hand, EIF4A3 manifests oncogenic characteristic via directly stabilizing the onco-lncRNAs. For example, EIF4A3 inhibited the degradation of LINC00680 and TTN-AS1 by binding to these lncRNAs, which were upregulated in glioblastoma cells. Ultimately, excess amount of LINC00680 and TTN-AS1 targeted miR-320b/EGR3/PKP2 axis to promote the development of glioblastoma.³⁵ In the present study, we proved that EIF4A3 bound to AGAP2-AS1 to prolong the half-life period of AGAP2-AS1, hence promoting the activation of MRC-5 cells. MyD88/NF- κ B signaling has not been investigated activating CAFs, but in organ fibrosis, including myocardial fibrosis,³⁶ liver fibrosis,^{37,38} kidney fibrosis,³⁹ and pulmonary fibrosis⁴⁰ the pro-fibrotic role is widely proved. In particular, the AGAP2-AS1/MyD88/NF- κ B axis was previously demonstrated in breast cancer,¹⁹ and EIF4A3/AGAP2-AS1/MyD88/NF- κ B signaling was proved to activate MRC-5 cells in the current study. Our findings are similar to the previous results and fill the knowledge gap of EIF4A3 functions in regulating the tumor microenvironment.

To sum up, our present results reveal the promotive role of AGAP2-AS1 in activating CAFs and confirm the EIF4A3/AGAP2-AS1/MyD88/NF- κ B axis, providing a novel strategy for LC therapy.

AUTHOR CONTRIBUTIONS

Conception and design: W.X. and Q.X. Performed the experiments: Q.X., H.H., T.Z., and J.F. Collection and assembly of data: Q.X., T.Z., H.H., and J.F. Data analysis and interpretation: Q.X., T.Z., and W.X. Manuscript writing: all authors. Final approval of manuscript: all authors.

ACKNOWLEDGMENTS

Not applicable.

CONFLICT OF INTEREST

The authors declare no conflict of interest.

DATA AVAILABILITY STATEMENT

The data obtained in this research are available from the corresponding author on reasonable request.

ORCID

Weiping Xie  <https://orcid.org/0000-0002-6011-0143>

REFERENCES

- Chen W, Zheng R, Baade PD, Zhang S, Zeng H, Bray F, et al. Cancer statistics in China, 2015. *CA Cancer J Clin.* 2016;66(2):115–32.
- Schabath MB, Cote ML. Cancer progress and priorities: lung cancer. *Cancer Epidemiol Biomarkers Prev.* 2019;28(10):1563–79.
- Xiang H, Ramil CP, Hai J, Zhang C, Wang H, Watkins AA, et al. Cancer-associated fibroblasts promote immunosuppression by inducing ROS-generating monocytic MDSCs in lung squamous cell carcinoma. *Cancer Immunol Res.* 2020;8(4):436–50.
- Piersma B, Hayward MK, Weaver VM. Fibrosis and cancer: a strained relationship. *Biochim Biophys Acta Rev Cancer.* 2020;1873(2):188356.
- Nurmik M, Ullmann P, Rodriguez F, Haan S, Letellier E. In search of definitions: cancer-associated fibroblasts and their markers. *Int J Cancer.* 2020;146(4):895–905.
- Miyai Y, Esaki N, Takahashi M, Enomoto A. Cancer-associated fibroblasts that restrain cancer progression: hypotheses and perspectives. *Cancer Sci.* 2020;111(4):1047–57.
- Costa A, Kieffer Y, Scholer-Dahirel A, Pelon F, Bourachot B, Cardon M, et al. Fibroblast heterogeneity and immunosuppressive environment in human breast cancer. *Cancer Cell.* 2018;33(3):463–479 e410.
- Chen X, Song E. Turning foes to friends: targeting cancer-associated fibroblasts. *Nat Rev Drug Discov.* 2019;18(2):99–115.
- Pegtel DM, Gould SJ. Exosomes. *Annu Rev Biochem.* 2019;88:487–514.
- Kalluri R, LeBleu VS. The biology, function, and biomedical applications of exosomes. *Science.* 2020;367(6478):1–40.
- Dai J, Su Y, Zhong S, Cong L, Liu B, Yang J, et al. Exosomes: key players in cancer and potential therapeutic strategy. *Signal Transduct Target Ther.* 2020;5(1):145.
- Yang X, Li Y, Zou L, Zhu Z. Role of exosomes in crosstalk between cancer-associated fibroblasts and cancer cells. *Front Oncol.* 2019; 9:356.
- Xu K, Zhang C, Du T, Gabriel ANA, Wang X, Li X, et al. Progress of exosomes in the diagnosis and treatment of lung cancer. *Biomed Pharmacother.* 2021;134:111111.
- Zhao T, Khadka VS, Deng Y. Identification of lncRNA biomarkers for lung cancer through integrative cross-platform data analyses. *Aging.* 2020;12(14):14506–27.
- Bhan A, Soleimani M, Mandal SS. Long noncoding RNA and cancer: a new paradigm. *Cancer Res.* 2017;77(15):3965–81.
- Qian X, Zhao J, Yeung PY, Zhang QC, Kwok CK. Revealing lncRNA structures and interactions by sequencing-based approaches. *Trends Biochem Sci.* 2019;44(1):33–52.
- Ferre F, Colantoni A, Helmer-Citterich M. Revealing protein-lncRNA interaction. *Brief Bioinform.* 2016;17(1):106–16.
- Tao Y, Tang Y, Yang Z, Wu F, Wang L, Yang L, et al. Exploration of serum exosomal lncRNA TBILA and AGAP2-AS1 as promising biomarkers for diagnosis of non-small cell lung cancer. *Int J Biol Sci.* 2020;16(3):471–82.
- Dong H, Wang W, Mo S, Chen R, Zou K, Han J, et al. SP1-induced lncRNA AGAP2-AS1 expression promotes chemoresistance of breast

- cancer by epigenetic regulation of MyD88. *J Exp Clin Cancer Res.* 2018;37(1):202.
20. Mao X, Xu J, Wang W, Liang C, Hua J, Liu J, et al. Crosstalk between cancer-associated fibroblasts and immune cells in the tumor microenvironment: new findings and future perspectives. *Mol Cancer.* 2021; 20(1):131.
 21. Kalluri R. The biology and function of fibroblasts in cancer. *Nat Rev Cancer.* 2016;16(9):582–98.
 22. Yang SS, Ma S, Dou H, Liu F, Zhang SY, Jiang C, et al. Breast cancer-derived exosomes regulate cell invasion and metastasis in breast cancer via miR-146a to activate cancer associated fibroblasts in tumor microenvironment. *Exp Cell Res.* 2020;391(2):111983.
 23. Fang T, Lv H, Lv G, Li T, Wang C, Han Q, et al. Tumor-derived exosomal miR-1247-3p induces cancer-associated fibroblast activation to foster lung metastasis of liver cancer. *Nat Commun.* 2018;9(1):191.
 24. Li W, Sun M, Zang C, Ma P, He J, Zhang M, et al. Upregulated long non-coding RNA AGAP2-AS1 represses LATS2 and KLF2 expression through interacting with EZH2 and LSD1 in non-small-cell lung cancer cells. *Cell Death Dis.* 2016;7:e2225.
 25. Liu Z, Wang Y, Wang L, Yao B, Sun L, Liu R, et al. Long non-coding RNA AGAP2-AS1, functioning as a competitive endogenous RNA, upregulates ANXA11 expression by sponging miR-16-5p and promotes proliferation and metastasis in hepatocellular carcinoma. *J Exp Clin Cancer Res.* 2019;38(1):194.
 26. Zheng Y, Lu S, Xu Y, Zheng J. Long non-coding RNA AGAP2-AS1 promotes the proliferation of glioma cells by sponging miR-15a/b-5p to upregulate the expression of HDGF and activating Wnt/beta-catenin signaling pathway. *Int J Biol Macromol.* 2019;128:521–30.
 27. Hong S, Yan Z, Song Y, Bi M, Li S. LncRNA AGAP2-AS1 augments cell viability and mobility, and confers gemcitabine resistance by inhibiting miR-497 in colorectal cancer. *Aging.* 2020;12(6):5183–94.
 28. Pascual-Marqui RD, Valdes-Sosa PA, Alvarez-Amador A. A parametric model for multichannel EEG spectra. *Int J Neurosci.* 1988;40(1–2): 89–99.
 29. Qi F, Liu X, Wu H, Yu X, Wei C, Huang X, et al. Long noncoding AGAP2-AS1 is activated by SP1 and promotes cell proliferation and invasion in gastric cancer. *J Hematol Oncol.* 2017;10(1):48.
 30. Hui B, Ji H, Xu Y, Wang J, Ma Z, Zhang C, et al. RREB1-induced upregulation of the lncRNA AGAP2-AS1 regulates the proliferation and migration of pancreatic cancer partly through suppressing ANKRD1 and ANGPTL4. *Cell Death Dis.* 2019;10(3):207.
 31. Kanellis DC, Espinoza JA, Zisi A, Sakkas E, Bartkova J, Katsori AM, et al. The exon-junction complex helicase eIF4A3 controls cell fate via coordinated regulation of ribosome biogenesis and translational output. *Sci Adv.* 2021;7(32):1–19.
 32. Song H, Liu Y, Li X, Chen S, Xie R, Chen D, et al. Long noncoding RNA CASC11 promotes hepatocarcinogenesis and HCC progression through EIF4A3-mediated E2F1 activation. *Clin Transl Med.* 2020; 10(7):e2220.
 33. Li Q, Lei C, Lu C, Wang J, Gao M, Gao W. LINC01232 exerts oncogenic activities in pancreatic adenocarcinoma via regulation of TM9SF2. *Cell Death Dis.* 2019;10(10):698.
 34. Yang H, Yang W, Dai W, Ma Y, Zhang G. LINC00667 promotes the proliferation, migration, and pathological angiogenesis in non-small cell lung cancer through stabilizing VEGFA by EIF4A3. *Cell Biol Int.* 2020;44(8):1671–80.
 35. Tang W, Wang D, Shao L, Liu X, Zheng J, Xue Y, et al. LINC00680 and TTN-AS1 stabilized by EIF4A3 promoted malignant biological behaviors of glioblastoma cells. *Mol Ther Nucleic Acids.* 2020;19: 905–21.
 36. Xu GR, Zhang C, Yang HX, Sun JH, Zhang Y, Yao TT, et al. Modified citrus pectin ameliorates myocardial fibrosis and inflammation via suppressing galectin-3 and TLR4/MyD88/NF-kappaB signaling pathway. *Biomed Pharmacother.* 2020;126:110071.
 37. Hu N, Wang C, Dai X, Zhou M, Gong L, Yu L, et al. Phillygenin inhibits LPS-induced activation and inflammation of LX2 cells by TLR4/MyD88/NF-kappaB signaling pathway. *J Ethnopharmacol.* 2020;248:112361.
 38. Hu N, Guo C, Dai X, Wang C, Gong L, Yu L, et al. Forsythiae Fructus water extract attenuates liver fibrosis via TLR4/MyD88/NF-kappaB and TGF-beta/smads signaling pathways. *J Ethnopharmacol.* 2020;262:113275.
 39. Ma JQ, Zhang YJ, Tian ZK, Liu CM. Bixin attenuates carbon tetrachloride induced oxidative stress, inflammation and fibrosis in kidney by regulating the Nrf2/TLR4/MyD88 and PPAR-gamma/TGF-beta1/Smad3 pathway. *Int Immunopharmacol.* 2021;90:107117.
 40. Li C, Yu Y, Li W, Liu B, Jiao X, Song X, et al. Phycocyanin attenuates pulmonary fibrosis via the TLR2-MyD88-NF-kappaB signaling pathway. *Sci Rep.* 2017;7(1):5843.

How to cite this article: Xu Q, Zhao T, Han H, Fan J, Xie W. EIF4A3 stabilizes the expression of lncRNA AGAP2-AS1 to activate cancer-associated fibroblasts via MyD88/NF- κ B signaling. *Thorac Cancer.* 2023; 14(5):450–61. <https://doi.org/10.1111/1759-7714.14762>